Configurational properties of polypyrrole chains

Ersin Yurtsever
Chemistry Department, Middle East Technical University, Ankara, Turkey

and Burak Erman*
Polymer Research Center, School of Engineering, Bogazici University and TUBITAK Advanced Polymeric Materials Research Center, Bebek 80815, Istanbul, Turkey
(Received 6 July 1992; revised 5 January 1993)

Conformational energy surfaces are determined as functions of torsional angles of bonds between rings for an α–α pyrrole trimer by using semiempirical quantum-mechanical calculations (AM1). Isomeric states for torsional rotations are identified as positions of minimum energy. Statistical weights determined on this basis are used in calculating the average dimensions of polypyrrole chains by the rotational isomeric state (RIS) model and the matrix multiplication scheme. Results of calculations indicate that the chains have unusually large characteristic ratios and persistence lengths with very strong temperature dependence. Characteristic ratios obtained by the RIS model show perfect agreement, in a wide temperature range, with the predictions of the worm-like chain model.

INTRODUCTION

Electronic properties and conformational behaviour of polypyrroles attract a great deal of attention owing to the high conductivity of polypyrroles upon doping[1–8]. Although pyrrole blacks have been known for a long time, thorough analysis of polypyrroles started with their first electrochemical synthesis[9]. Owing to their high environmental stabilities, a large number of technological applications of polypyrroles have been proposed[10–13].

Chain organization and morphology in the solid polypyrrole are of major importance in determining both the processability and the conductivity of the material. The semicrystalline structure of the solid polypyrrole results from the relatively high persistence length of the single chains. In fact, the departure of the angle between two successive backbone C–C bonds (ca 44°, see below) from that obtained in the near-tetrahedral bond angle of common polymers results, as in the case of the aromatic polyamides and polyesters, in a high degree of persistence of the end-to-end vector. The stiffness of these chains resulting from the near alignment of the successive bonds may be termed as the 'geometric stiffness', as opposed to the 'energetic stiffness' that obtains in chains with very high energy barriers to rotameric transitions.

In the present paper, we study the configurational features of the single polypyrrole chain. The persistence vector and the characteristic ratio of the chain are obtained by adopting the matrix multiplication scheme and the rotational isomeric state (RIS) method[14,15]. The organization of the paper is as follows. In the theory section the structure of the chain and torsional energy maps are obtained by quantum-mechanical, semiempirical calculations, followed by rotational isomeric state calculations of the end-to-end dimensions. Values of the mean-square end-to-end distance and the vector components of the end-to-end vector are presented in the following section as a function of temperature and the number of repeat units. In the final section the correspondence of the single polypyrrole chain to the worm-like chain model is discussed.

THEORY

Structure of the trimer and torsional energy surfaces

The majority of quantum-mechanical calculations on the structures of oligomers of pyrroles and derivatives are based on a semiempirical methodology. The high number of possible rotational and conformational isomers makes a detailed analysis of the *ab initio* potential hypersurface very difficult. On the other hand, semiempirical calculations at the AM1 level[16] have been shown to produce quite reliable descriptions of the bonding in heterocyclic compounds. In all of the present calculations, the AM1 option of MOPAC[17] was used with a graphics interface to the molecular-modelling program MOLCAD[18]. The graphics interface allows a simple investigation of the initial input, thereby eliminating the costly study of a large number of sterically improbable structures.

The structures of the pyrrole monomer and α–α bipyrrole are obtained by optimizing all parameters. The torsional map is computed by relaxing six parameters for each bond (one distance, two valencies and three
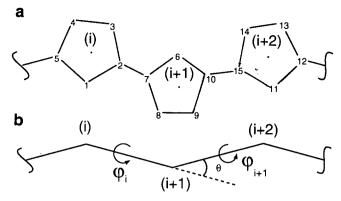
a

b

Figure 1 (a) The structure of the trimer. The labels i, $i+1$ and $i+2$ in parentheses locate the centre of each ring. (b) Representation of the chain as a succession of virtual bonds. θ is the bond angle. The angles φ_i and φ_{i+1} represent the torsional angles

Table 1 Structural data for the trimer

Atom number	Position (Å)		
	x	y	z
1	0.000	0.000	0.000
2	1.088	0.816	−0.333
3	0.685	2.158	−0.0203
4	−0.686	2.150	0.221
5	−1.078	0.810	0.337
6	3.452	1.099	−1.062
7	2.364	0.281	−0.729
8	2.767	−1.064	−0.863
9	4.137	−1.064	−1.267
10	4.583	0.282	−1.390
11	6.908	0.001	−2.104
12	7.994	0.821	−2.422
13	7.599	2.158	−2.291
14	6.227	2.160	−1.884
15	5.818	0.817	−1.775

torsional angles) while keeping the other geometrical parameters frozen. A small number of calculations optimizing the full $3N$-dimensional space did not produce any significantly different results.

The structure of the trimer is shown in *Figure 1a*. The labels i, $i+1$ and $i+2$ in parentheses locate the centre of each ring. Atoms on the ring are numbered in a counter-clockwise fashion. Nitrogen atoms in the rings are labelled as 1, 6 and 11. The position of each labelled atom in the figure, relative to the first nitrogen atom, is given in *Table 1*. Calculations based on these coordinates show that the rings are very close to planar. The angle between the planes 6–10–9 and 7–6–10, for example, is 0.086°. The angle between the unit normals of the planes formed by atoms 1–2–3 and 6–7–8 is less than 1°. The angle between the plane of the atoms 9–10–11 and bond 10–15 is about 4°. These calculations indicate that the minimum energy configuration of the molecules shown in *Figure 1a* is not parallel to the xy plane. The deviations from planar geometry are not significant, however. In the interest of simplifying the calculations of chain statistics, the indicated minimum energy conformation of the molecule is assumed to be planar. Within the validity of this assumption, bonds 2–7 and 10–15 intersect at the point $(i+1)$. The molecule may thus be represented as a sequence of virtual bonds joining the centres of the rings, as shown in *Figure 1b*. These virtual bonds, each of length 3.88 Å, represent axes about which torsional rotations of the rings take place. The angle θ (*Figure 1b*) formed by

two successive virtual bond vectors is 43.6°. This value of the bond angle is much smaller than the bond angles of common flexible polymers. The bond angle for polyethylene is 68°, for example. The angles φ_i and φ_{i+1} in *Figure 1b* represent the torsional angles.

The energy surface or the contour map generated by rotations φ_i and φ_{i+1} is shown in *Figure 2*. Only half of the full diagram is shown because of its symmetry, i.e. the other half may be obtained upon inversion through the origin. Contour lines are drawn at 0.4 kcal (1 cal = 4.2 J) intervals. The location of minimum energy is at $0°, 0°)$ and is chosen as the *trans–trans* (tt) state. The *trans–gauche*$^+$ (tg^+) minimum is located at $(0°, 150°)$ and has an energy of 0.79 kcal mol^{-1} relative to the tt minimum. The *trans–gauche*$^-$ (tg^-) minimum of 0.79 kcal mol^{-1} is similarly calculated at $(0°, -150°)$. Owing to errors in optimization a slight asymmetry is observed along the $\varphi_i = 0°$ line, and this is ignored in the calculations that follow. The minima for the g^+g^+ and g^+g^- states with energies of 2.05 kcal mol^{-1} are located at $(150°, 150°)$ and $(150°, -150°)$, respectively. The g^+t state is at $(150°, 0°)$ and has an energy of 0.79 kcal mol^{-1}. Two relatively sharp peaks of about 3.4 kcal mol^{-1} are observed in the vicinity of $(90°, \pm 90°)$. The energy map is presented in *Figure 3* in three dimensions. The g^+g^+ and g^+g^- states are very shallow, as can be seen in this figure.

The results of the present calculations are in approximate agreement with the molecular mechanics
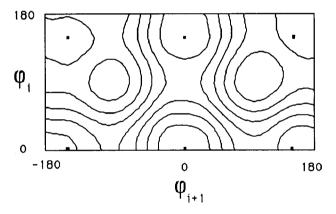
Figure 2 Energy surface generated by rotations φ_i and φ_{i+1}. Only half of the full diagram is shown as the other half may be obtained upon inversion through the origin. Contour lines are drawn at 0.4 kcal intervals
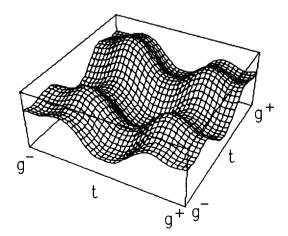
Figure 3 Three-dimensional representation of the energy map

calculations by Orchard *et al.*[4] with some minor differences. The energies of the $tg^{\pm}$ states, 0.79 kcal mol^{-1}, are the same in the two studies. The present analysis locates the *gauche* state at 150° relative to the *trans*, whereas the work of Orchard *et al.* locates it at 180°. The sharp peaks of about 3.4 kcal mol^{-1} in the vicinity of (90°, ±90°) are calculated by Orchard *et al.* to be about 4.3 kcal mol^{-1} at the same location.

Statistical weight matrices

The energy $E_{\zeta\eta}$ of bond $i+1$ in state η when bond i is in state ζ is required for the evaluation of the statistical weight matrices[14] for the bond pair. Assuming that interactions between non-bonded atoms are negligible in the tg^{+} state, the 0.79 kcal mol^{-1} energy of the tg^{+} state is assigned to the intrinsic rotational barrier about individual bonds. With this assignment, the energy matrix $E_{\zeta\eta}$ is obtained in kcal mol^{-1} as

$$E_{\zeta\eta} = \begin{matrix} & t & g^{+} & g^{-} \\ t \\ g^{+} \\ g^{-} \end{matrix} \begin{bmatrix} 0 & 0.79 & 0.79 \\ 0 & 1.26 & 1.26 \\ 0 & 1.26 & 1.26 \end{bmatrix} \tag{1}$$

The $\zeta\eta$ element $u_{\zeta\eta}$ of the statistical weight matrix **U** is given as $u_{\zeta\eta} = \exp(-E_{\zeta\eta}/RT)$. At 300 K, for example, the matrix takes the form

$$\mathbf{U} = \begin{bmatrix} 1 & 0.266 & 0.266 \\ 1 & 0.121 & 0.121 \\ 1 & 0.121 & 0.121 \end{bmatrix} \tag{2}$$

Calculation of averages

The average dimensions of a chain of n virtual bonds may be calculated following the matrix multiplication scheme given elsewhere[14,15]. The procedure is briefly outlined in the present section.

The partition function Z for a chain of n bonds is

$$Z = \mathbf{U}_1^{(n)} \tag{3}$$

The right-hand side of equation (3) represents the serial product of the statistical weight matrices. The subscript 1 and the superscript n indicate that the multiplication starts from the first and ends at the nth bond.

The generator matrix $\mathbf{A}_i$ for calculating the average end-to-end vector $\langle \mathbf{r} \rangle$ is

$$\mathbf{A}_i = \begin{bmatrix} \mathbf{T} & \mathbf{l} \\ 0 & 1 \end{bmatrix} \tag{4}$$

Here, the subscript i locates the position of the bond along the chain. **T** is the transformation matrix[14] that transforms a vector in coordinate frame $i+1$ to the ith frame and **l** is the bond vector. The coordinate system for each bond is chosen as given by Flory. The first and last bonds are assumed to be in the *trans* state. A laboratory-fixed coordinate system is assumed such that the x axis is parallel to the first bond and the xy plane contains the first two bonds.

The generator matrix $\mathbf{G}_i$ for calculating the unperturbed mean-square end-to-end distance $\langle r^2 \rangle_0$ is

$$\mathbf{G}_i = \begin{bmatrix} 1 & 2\mathbf{l}^T\mathbf{T} & l^2 \\ 0 & \mathbf{T} & \mathbf{l} \\ 0 & 0 & 1 \end{bmatrix} \tag{5}$$

where l is the magnitude of **l** and the superscript T denotes the transpose.

The statistical average $\langle f \rangle$ of any quantity f is obtained as

$$\langle f \rangle = \mathscr{F}_{[1} \mathscr{F}_2^{(n-2)} \mathscr{F}_{n]} Z^{-1} \tag{6}$$

In the present study, f stands either for **r** or r^2. The matrices $\mathscr{F}$ are defined as

$$\mathscr{F}_{[1} = [\mathbf{F}_{[1} \quad 0 \quad 0 \quad \dots \quad 0]$$

$$\mathscr{F}_{n]} = \text{col}(\mathbf{F}_{n]} \quad \mathbf{F}_{n]} \quad \dots \mathbf{F}_{n]}) \tag{7}$$

$$\mathscr{F}_i = (\mathbf{U}_i \otimes \mathbf{E}_s) \| \mathbf{F}_i \| \qquad 1 < i < n$$

where the matrix **F** represents the generator matrix **A** for **r** or **G** for r^2. $\mathbf{F}_{[1}$ and $\mathbf{F}_{n]}$ are the first row and the last column of $\mathbf{F}_1$ and $\mathbf{F}_n$, respectively. $\mathbf{E}_s$ is the identity matrix of dimension s. $\| \mathbf{F}_i \|$ is the diagonal array of the generator matrix for each of the t, g^{+} and g^{-} states.

RESULTS OF CALCULATIONS

The averages $\langle r^2 \rangle_0$ and $\langle r \rangle$ for the polypyrrole chain were calculated according to the general matrix multiplication scheme outlined in the preceding section. All calculations were performed for $T = 200, 250, 300, 350, 400$ and 450 K. In *Figure 4*, the dependence of $\langle r^2 \rangle_0$ on the number of virtual bonds is shown. The curves from top to bottom are in ascending order of temperature, the highest curve being obtained for 200 K and the lowest for 450 K. The dependence of $\langle r^2 \rangle_0$, or the characteristic ratio C_n, defined as

$$C_n = \langle r^2 \rangle_0 / nl^2 \tag{8}$$

on temperature is very strong, as can be seen from the figure. The limiting values of C_n for large n, represented as C_∞, are given in the first row of *Table 2* as a function of temperature. The temperature coefficient of the mean-square end-to-end distance, defined as $d \ln\langle r^2 \rangle_0 / dT$, is obtained for the infinitely long chain from *Figure 5* as -3.69×10^{-3} deg^{-1}. Since the data points do not lie on a straight line, only three points in the temperature range $350\,\text{K} < T < 450\,\text{K}$ are adopted in calculating the
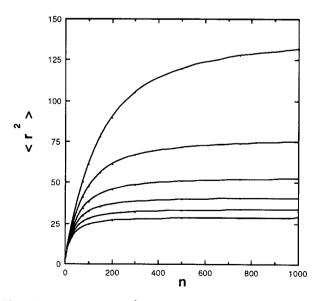

Figure 4 Dependence of $\langle r^2 \rangle_0$ on the number of virtual bonds. The curves from top to bottom are in ascending order of temperature, respectively, for 200, 250, 300, 350, 400 and 450 K

temperature coefficient. The value of the temperature coefficient obtained in this manner is more than three times larger than the temperature coefficient of polyethylene in the same temperature range.

The dependence of the average value $\langle x \rangle$ of the x component of the end-to-end vector on chain length is shown in *Figure 6*. The x direction represents the direction of the first bond. Values of $\langle x \rangle$ decrease monotonously

Table 2 Characteristic ratio and the average end-to-end vector for the infinitely long chain

	Temperature (K)					
	200	250	300	350	400	450
C_∞	139.1	77.3	53.5	41.3	33.8	28.6
$\langle x \rangle$	269.8	148.5	102.5	79.2	65.0	55.4
$\langle y \rangle$	112.3	64.1	46.0	36.9	31.4	27.6
r/l	75.3	41.7	29.0	22.5	18.6	16.0
m'	161.4	89.3	62.0	47.9	39.2	33.1

Figure 7 Dependence of the average value $\langle y \rangle$ of the y component of the end-to-end vector on chain length. See legend for *Figure 4* for the temperatures
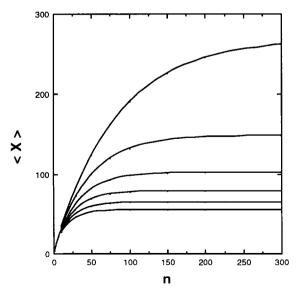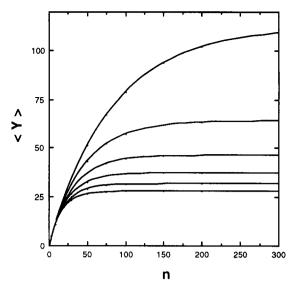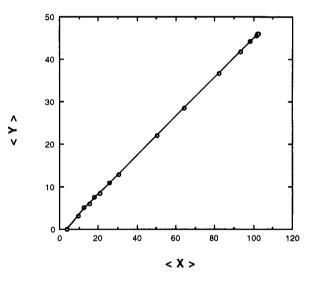

Figure 5 Temperature coefficient of the mean-square end-to-end distance for the infinitely long chain

Figure 8 The x and y components of the persistence vector at $T = 300$ K

with decreasing temperature. Their limiting values for the infinitely long chain are given in the second row of *Table 2*. The averages $\langle y \rangle$ are shown in *Figure 7* and their limiting values for the infinitely long chain are given in the third row of *Table 2*. The average of the z component of the end-to-end vector equates to zero owing to the assumed symmetry of the chain about the xy plane.

The average vector $\langle \mathbf{r} \rangle$ may be defined as the persistence vector, whose magnitude is a measure of the stiffness of the chain[19]. The x and y components of the persistence vector at $T = 300$ K are shown in *Figure 8*. The persistence vector lies in the plane of the first two bonds, owing to symmetry, and makes an angle of about 25° with the first bond. Its direction is approximately independent of chain length, as can be seen from the figure. At this temperature, the persistence vector is about 112 Å. This is significantly larger than that of polyethylene[19]*, which is of the order of 7.5 Å at

Figure 6 Dependence of the average value $\langle x \rangle$ of the x component of the end-to-end vector on chain length. See legend for *Figure 4* for the temperatures

* The present definition of the persistence vector, adopted following Flory and Yoon, differs from the more widely used definition which takes up only the x component as the persistence vector.

comparable temperatures. The values of the persistence vector length calculated from the second and third rows of *Table 2* divided by the length of a repeat unit ($l = 3.88$ Å) are given in the fourth row of *Table 2*. These values fall significantly below the predictions of Rossi et al.[20]. The origin of the disagreement is explained in the Conclusions and Discussion section.

CORRELATION WITH THE FREELY JOINTED AND THE WORM-LIKE CHAIN

Correlation with the freely jointed chain is established[14] in the limit of the infinitely long chain by the usual method of equating (i) the mean-squared values $\langle r^2 \rangle$ and (ii) the stretched end-to-end lengths of the real and the hypothetical freely jointed chains. Two equations obtained in this manner yield the length l' and the number n' of segments of the equivalent freely jointed chain as

$$l' = \frac{C_\infty}{\cos(\theta/2)} l \tag{9}$$

and

$$n' = \frac{\cos^2(\theta/2)}{C_\infty} n \tag{10}$$

The number of bonds m' in a freely jointed segment is obtained from equation (10) as

$$m' = \frac{C_\infty}{\cos^2(\theta/2)} \tag{11}$$

Values of m' calculated according to equation (11) are given in the fifth row of *Table 2* as a function of temperature. The values of m' vary from 161.4 at 200 K to 33.1 at 450 K. These values are much larger than that of the polyethylene chain, which is about 10 at 400 K. These calculations indicate that the polypyrrole chain may be classified as a semiflexible or worm-like chain.

The worm-like chain[14] is an approximate and simple model which may represent the behaviour of semiflexible chains, and is used to advantage in analytical calculations of chain statistics. It is characterized by two length parameters, L and a, defined in terms of the variables used for the real chain as

$$L = r_{max} = nl \cos(\theta/2) \tag{12}$$

and

$$a = \frac{C_\infty}{2 \cos^2(\theta/2)} l \tag{13}$$

where r_{max} is the stretched length of the chain. The characteristic ratio C_n of the real chain is expressed in terms of the two parameters L and a of the worm-like chain as

$$C_n = C_\infty \left[1 - \frac{1 - \exp(-L/a)}{L/a} \right] \tag{14}$$

In *Figure 9*, values of C_n calculated according to equation (14) (solid curves) are compared with the results of matrix multiplication calculations (empty circles) for the real chain. Comparison at the three temperatures 200 K (upper curve), 300 K (middle curve) and 400 K (lower curve) indicates excellent agreement, pointing to the fact that a semiflexible chain such as polypyrrole may safely be treated according to the worm-like chain model.
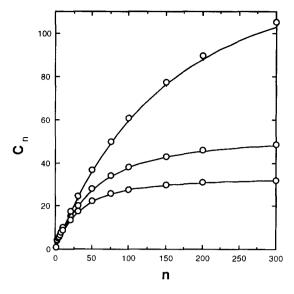

Figure 9 Values of C_n calculated according to equation (14) (solid curves). The circles represent the results of matrix multiplication calculations for the real chain. Comparison is made between the results at three different temperatures: 200 K (upper curve), 300 K (middle curve) and 400 K (lower curve)
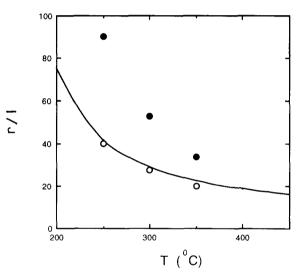

Figure 10 Comparison of the calculated persistence length values with those from the work of Rossi et al.[20] as a function of temperature. The solid curve is from the present calculations and the filled circles are from the work of Rossi et al. The empty circles were also obtained by Rossi et al. for equal *trans* and *gauche* energies

CONCLUSIONS AND DISCUSSION

The dimensions of the individual polypyrrole chain exhibit unusually large values and very strong dependence on temperature. The unusually high values of chain dimensions result both from the significant departure of the successive backbone bonds from the tetrahedral structure and from very high energy barriers between rotational isomeric minima. The latter factor is especially important in slowing down the local dynamics of the single chain by diminishing the transition rates from one isomeric state to the other.

The torsional energy maps obtained in the present work are also closely predicted in the calculations of Orchard et al.[4], as described earlier. Our calculations of the persistence vectors based on these energy maps are in disagreement with those obtained in a recent study by Rossi et al.[20]. In *Figure 10* the values of r/l, where r is
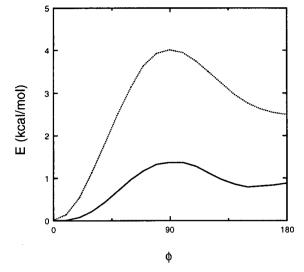
Figure 11 Torsional energy values used in the present work (solid curve) and by Rossi *et al.*[20] (dotted curve)

the magnitude of the persistence length and *l* is the length (3.88 Å) of the virtual bond, are presented as a function of temperature and compared with the results of calculations by Rossi *et al.* The solid curve is from the present study and the filled circles are from the work of Rossi *et al.* Their results were obtained from torsional energy maps based on the values given by Bredas *et al.*[21]. The data (empty circles) in *Figure 10* were obtained by Rossi *et al.* by equating the value of the *gauche* state energy to that of the *trans*. In *Figure 11*, the torsional energies of the present work are compared with those of Rossi *et al.* The energy of the *gauche* state is obtained as 2.5 kcal mol^{-1} by Rossi *et al.*, while it is 0.79 kcal mol^{-1} according to Orchard *et al.*[4] and the present work. A higher value of the *gauche* state energy increases the number of *trans* states and results in larger values of the persistence length. The strong temperature dependence of the persistence vector predicted both by Rossi *et al.* and the present work results from the unusually small value of the bond angle and the occurrence of the *gauche* state around ±170°.

REFERENCES

1   Street, G. B., Clarke, T. C., Geiss, R. H., Lee, V. Z., Nazzal, A., Pfluger, P. and Scott, J. C. *J. de Physique* 1983, **C3**, 599
2   Andre, J. M., Vercauteren, D. P., Street, G. B. and Bredas, J. L. *J. Chem. Phys.* 1984, **80**, 5643
3   Orti, E., Sanchez-Marin, J. and Tomas, F. *J. Mol. Struct. Theocem* 1985, **124**, 307
4   Orchard, B. J., Freidenreich, B. and Tripathy, S. *Polymer* 1986, **27**, 1533
5   Orti, E., Sanchez-Marin, J. and Tomas, F. *Theor. Chim. Acta* 1986, **69**, 41
6   Toussant, J. M., Themans, B., Andre, J. M. and Bredas, J. L. *Synth. Met.* 1989, **28**, C205
7   Bogang, T. and Zerbi, G. *Synth. Met.* 1989, **28**, C1
8   Yurtsever, E., Toppare, L. and Hallensleben, M. *J. Mol. Struct. Theocem* 1993, **280**, 1
9   Diaz, A., Kanazawa, K. K. and Gardini, G. P. *J. Chem. Soc., Chem. Commun.* 1979, **10**, 635
10   Burgmayer, P. and Mayer, R. W. *J. Chem. Phys.* 1984, **88**, 2515
11   Skotheim, T. J., Lundstrom, I. and Prezja, J. *J. Electrochem. Soc.* 1981, **128**, 1625
12   Skotheim, T. J., Peterson, L. G., Inganas, O. and Lundstrom, I. J. *J. Electrochem. Soc.* 1982, **129**, 1737
13   Cagnolati, R., Lucchesi, M., Rolla, P. A., Castelvetro, V., Ciardelli, F. and Colligiani, A. *Synth. Met.* 1992, in press
14   Flory, P. J. 'Statistical Mechanics of Chain Molecules', Interscience, New York, 1963, pp. 49–93
15   Flory, P. J. *Macromolecules* 1974, **7**, 381
16   Dewar, M. J. S., Zoeliste, E. G., Heady, E. F. and Stewart, J. J. P. *J. Am. Chem. Soc.* 1985, **107**, 3902
17   MOPAC version 5.00, QCPE # 455
18   Heiden, W., Schlrenkrich, M. and Brickmann, J. *J. Computer-Aided Mol. Des.* 1990, **4**, 255
19   Flory, P. J. and Yoon, D. Y. *J. Chem. Phys.* 1974, **61**, 5358
20   Rossi, G., Chance, R. R. and Silbey, R. *J. Chem. Phys.* 1989, **90**, 7594
21   Bredas, J. L., Street, G. B., Themans, B. and Andre, J. M. *J. Chem. Phys.* 1985, **83**, 1323